

Robust Route to Efficient Extraction of Cr from Different Cr-containing Hazardous Wastes by Capitalizing on a Reduction-chlorination-volatility Technique

Xueming Liu ^b, Jiaqing He ^a, Feng Gao ^a, Jin Zhou ^b, Xiaofeng Mo ^b, Zhen Wu ^b, Jiawei Lin ^b, Shi Wang ^c, Mengye Wang ^{a,*}, and Zhang Lin ^b

^a State Key Laboratory of Optoelectronic Materials and Technologies, School of Materials, Sun Yat-Sen University, Guangzhou 510275, PR China.

^b School of Environment and Energy, Key Laboratory of Pollution Control and Ecosystem Restoration in Industry Clusters (Ministry of Education), South China University of Technology, Guangzhou 510006, PR China.

^c Dongjiang Environmental Co. Ltd., Shenzhen 518000, PR China.

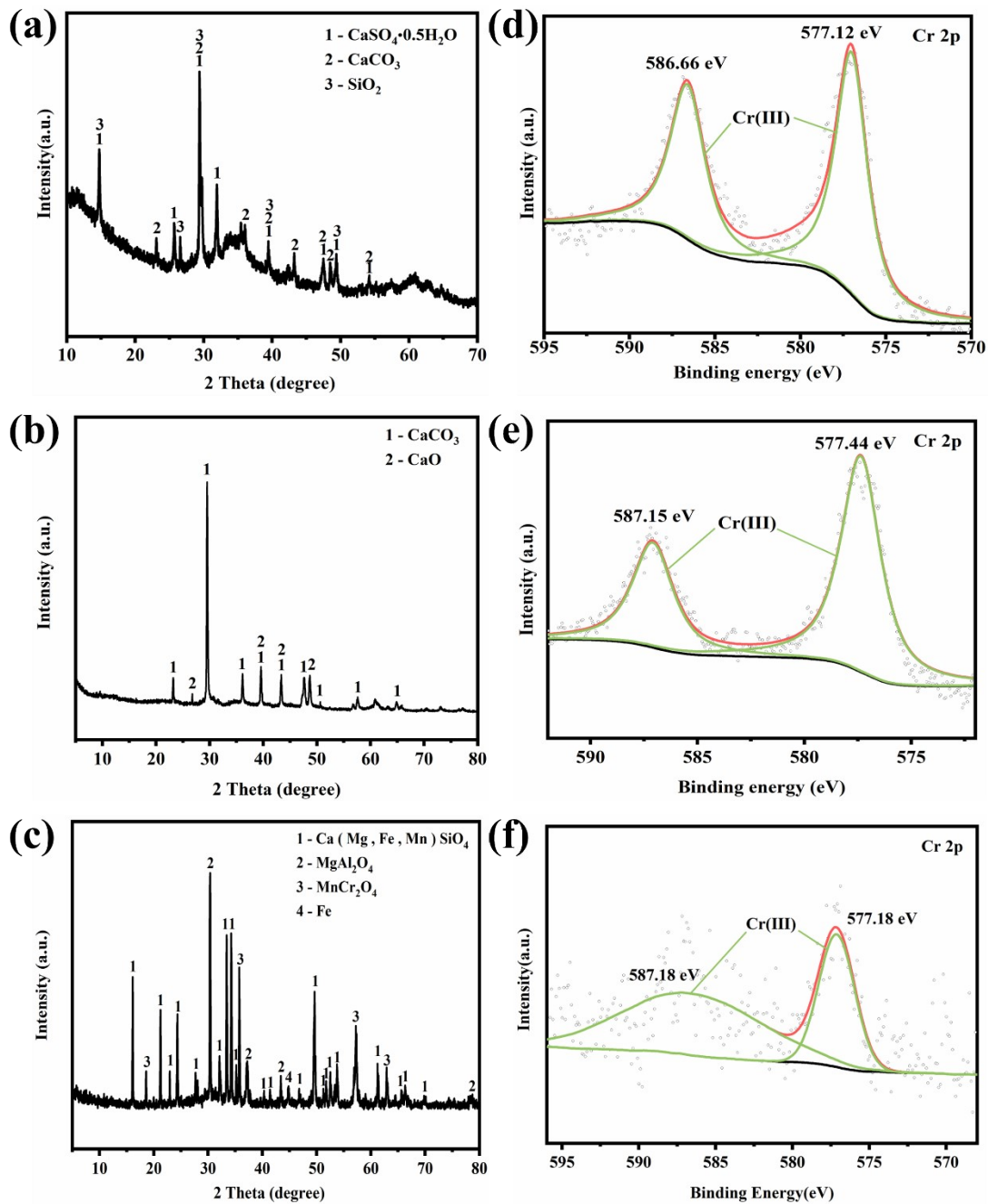


Fig. S1 XRD patterns of (a) ES; (b) TS and (c) SSS. High-resolution XPS spectra of Cr 2p in (d) ES, (e) TS and (f) SSS.

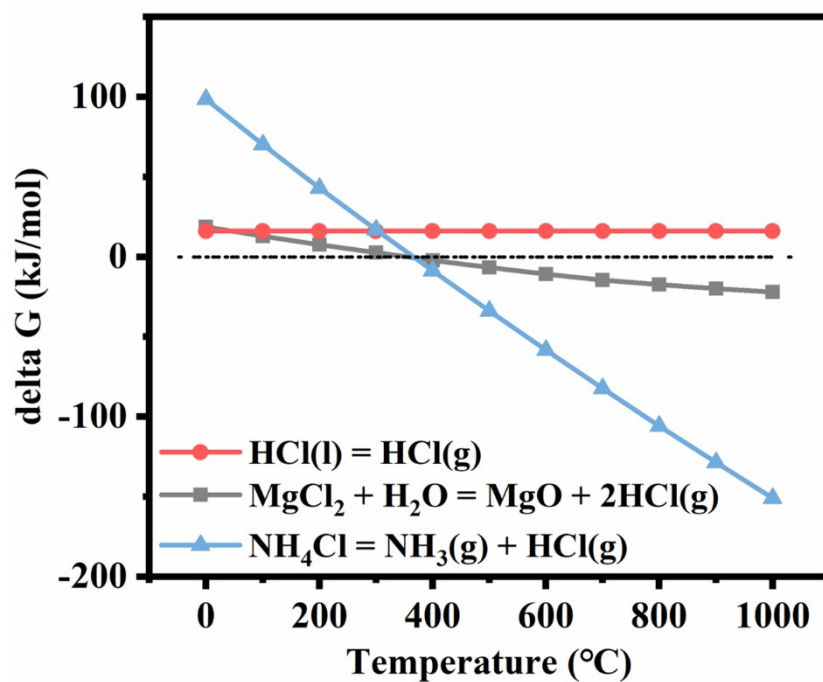


Fig. S2 Gibbs free energy of decomposition of the $\text{MgCl}_2 \cdot 6\text{H}_2\text{O}$, HCl and NH_4Cl at different temperatures.

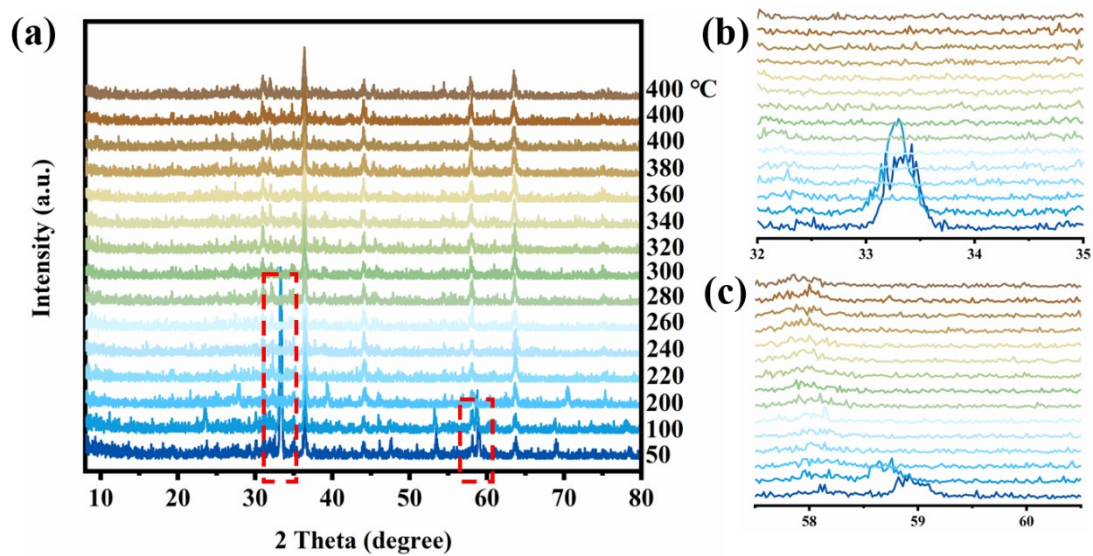


Fig. S3 (a) In situ XRD spectra of the mixed COPR and NH_4Cl at the temperature ranging from 50 to 400 °C. Enlarged spectra ranging from (b) 32°-35° and (c) 57.5°-60.5° part in (a).

Table S1. Activation energy of $\text{CrCl}_3 \cdot 6\text{H}_2\text{O}$ volatilization calculated by FWO method.

| α | R^2 | E_a (kJ/mol) |
|----------------|-------|----------------|
| 0.2 | 0.984 | 73.72 |
| 0.3 | 0.996 | 164.38 |
| 0.4 | 0.999 | 225.33 |
| 0.5 | 0.930 | 222.65 |
| 0.6 | 0.964 | 1696.43 |
| 0.7 | 0.419 | 278.48 |
| 0.8 | 0.889 | 255.12 |
| 0.9 | 0.939 | 205.36 |
| Average | - | 390.18 |

Table S2. Kinetic mechanism function and standard deviation.

| No. | reaction model | standard deviation |
|-----|------------------------------|--------------------|
| 1 | Avrami-Erofeev, m=4 | 1.120 |
| 2 | Avrami-Erofeev, m=3 | 1.679 |
| 3 | Avrami-Erofeev, m=2 | 0.175 |
| 4 | Avrami-Erofeev, m=1.5 | 2.206 |
| 5 | Phase boundary reaction, n=1 | 0.187 |
| 6 | Phase boundary reaction, n=2 | 2.834 |
| 7 | Phase boundary reaction, n=3 | 2.002 |
| 8 | One-dimensional diffusion | 0.846 |
| 9 | Two-dimensional diffusion | 8.977 |
| 10 | Three-dimensional diffusion | 0.159 |
| 11 | Jander' type diffusion | 0.140 |
| 12 | Power law, n=1/4 | 0.164 |
| 13 | Power law, n=1/3 | 0.249 |
| 14 | Power law, n=1/2 | 0.455 |
| 15 | Power law, n=2/3 | 0.578 |
| 16 | First order | 1.028 |

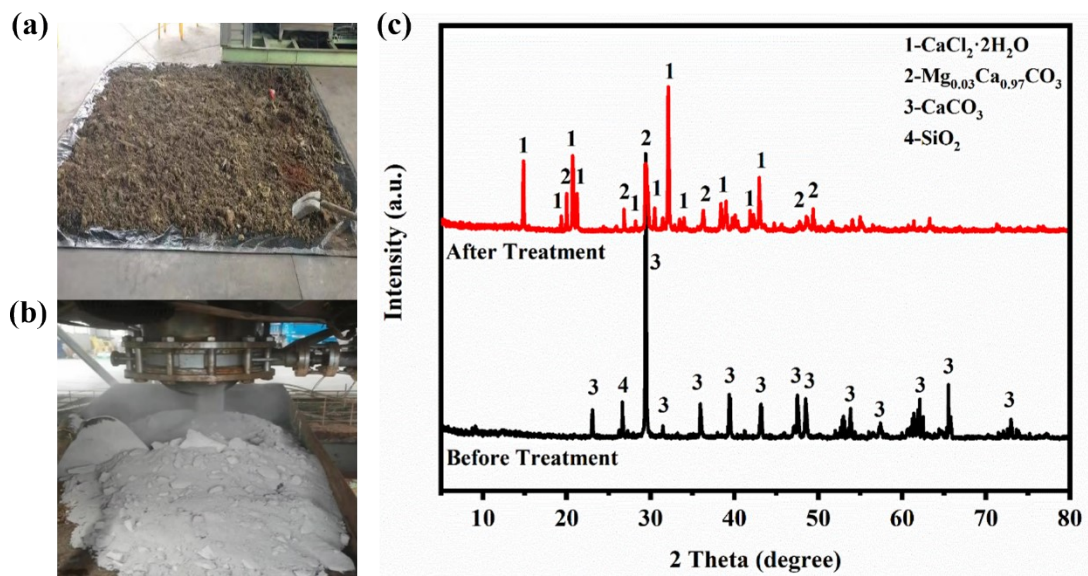


Fig. S4 Digital images (a) before and (b) after the pilot reaction. (c) XRD patterns of COPR before and after the pilot reaction.


| | | | | |
|-------------------|---|---|--|---|
| Powder |  |  |  |  |
| Leaching solution |  |  |  |  |

Fig. S5 Digital images of raw residues and leaching solution of powders after extracting Cr in three repeated pilot tests.

Table S3. Cr extraction rates of three Cr-containing wastes after the chlorination treatment.

| Types | Treatment | Extraction rate of Cr |
|--------------|------------------------------|------------------------------|
| ES | Chlorination + acid leaching | 82.1% |
| TS | Chlorination | 85.3% |
| SSS | Chlorination + acid leaching | 93.1% |

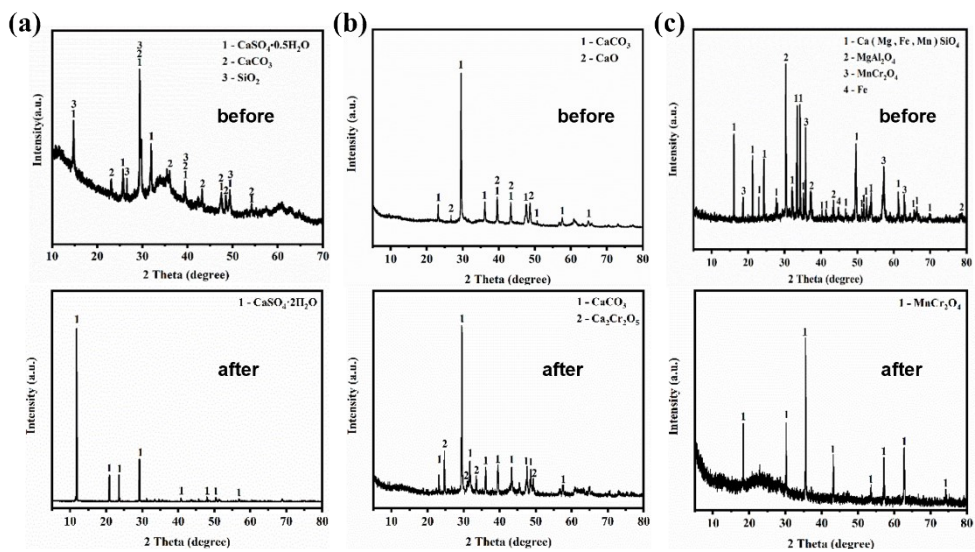


Fig. S6 XRD patterns of (a) ES, (b) TS and (c) SSS before and after the chlorination treatment.